Biomechanics, Vol. 29, No. 1, 2017 DOI: 10.1111/j.1539-6924.2009.01135.x

Verification of slice models of mammalian brains in transient dynamics

C. Duñó [1*] , P. Saez[2] , P. Diez[2] , F. Casadei[3]

To date, the brain remains the most intriguing and unexplored organ in humans. Although the vast majority of research is focused on understanding the way the brain functions at different spatial and temporal scales, an accurate characterisation of the mechanical behavior is fundamental for analysing the brain, because while mechanical stimuli are small under physiological conditions, mechanics have relevance in pathological conditions, including brain deformation or swelling such as brain tumor, brain injury and brain surgery. Well calibrated and validated constitutive models for brain tissue are essential to accurately simulate these phenomena, being the goal of these project to advance in these field, mainly in the dynamics aspects. In these report a 3D finite element reconstruction of the rat brain will be carried alongside with the verification of using a 3D thin slices of the rat brain geometry simplification, using the Abaqus commercial software.

KEY WORDS: Finite element method, Biomechanics, Hyperelastic modelling, Viscoelasticity.

1. INTRODUCTION

The head is often considered the most vulnerable part of the body and, in consequence the injuries to it have severe consequences or are even life-threatening. So, understanding its mechanical behavior is crucial for the study of brain diseases involving brain deformation or swelling such as brain tumor, strokes as well as the phenomena arising from traumatic brain injury. To develop preventive strategies for these injuries or even to provide doctors with valuable information for the treatment a finite element (FE) simulation have been proposed for the prediction of injuries.

The prototype example of these pathologies is the Traumatic Brain Injury (TBI) also known as intracranial injury, is a complex injury associated with a broad spectrum of symptoms and disabilities, and its caused by an external mechanical stimulus to the head such as a high acceleration, an impact or a blast. The range of effect of this pathology embraces from a focal damage of the brain tissue to a widespread axonal injury.[(1,2)]

One of the most common and complex pathological features of the TBI is the Diffuse Axonal Injury (DAI) which occurs in the white matter in a cellular level, not visible with conventional medical imaging modalities and it makes it difficult to diagnose. In these cases the computational models can help in capture the localization and the level of axonal damage, being a big help to the doctors.

Also, the relation of the mechanical strain and the death of the cells is much more complex tan it might be think, due to the multiple levels in which occurs, in a macroscopic level (organ) in a mesoscopic level (tissue), microscopic level (cell) and in a nanoscopic level (molecule)[(5)]. And due to that it cannot be predicted with only the typical stress strain rate criterion, a complete and accurate picture of the mechanical properties of the brain is needed.

[1]MSc Numerical Methods in Engineering, CIMNE - Universitat Politcnica de Catalunya, Barcelona, carles.duno@upc.edu
[2]UPC Barcelona - LaCàN
[3]Retired from JRC ELSA
[*]JRC Ispra

0272-4332/17/0100-0001$22.00/1

1.1 Brain Mechanics

The brain floats within the skull surrounded by the cerebrospinal fluid (CSF) which allows the relative motion between them.

Visually, the interior of the brain consists of an outer layer of the so-called grey matter (or gray matter) being the major component of the central nervous system, consisting principally of neuronal cell bodies, and a inner core of white matter consisting of an organized arrangement of neural axons, with a lighter color.

Prange and Margulies [12] concluded that white and gray matter have different physical properties, while gray matter was nearly isotropic, the white matter behavior was more anisotropic specifically, where fibers are well aligned, white matter is expected to be transversely isotropic with the fiber axis normal to the plane of isotropy, in both extension and shear [3,7].

Brain tissue is known to exhibit viscoelastic behavior, so, and with the previous, the constitutive model for the brain tissue will be extended to include linear viscoelasticity and fiber dispersion.

In a soft hyperelastic material like the brain, the exterior geometry (skull shape) have notorious implications in the outcome of the deformation or the velocity field.

1.2 Explicit dynamic analysis

The analysis will be carried in transient dynamics with geometric non-linearity, so an explicit in time integration can be taken into account to perform a stress/displacement analysis.

1.3 Numerical methods and models

For the analysis a finite elements simulations will be conducted using an explicit time integration scheme in the Abaqus 6.14 commercial software package. Because of the high computational cost of the whole 3D model, a 3D thin slice of the brain are used, and due to the high constrained nature of the brain tissue in the skull, a plane strain condition is considered for the 3D FE models of the slices.

As can be seen in the figure 1 a linear deceleration with initial velocity $V_0 = 0{,}1 m/s$ at the initial time $t_0 = 0s$ down to $0{,}0 m/s$ at $t_1 = 25ms$, followed by an imposed zero velocity until the chosen final time of $t_f = 50ms$, being able to simulate an impact to the head, without modeling the full neck [6], which would introduce rotation, neither the skull considering the nodes in the shape fixed.

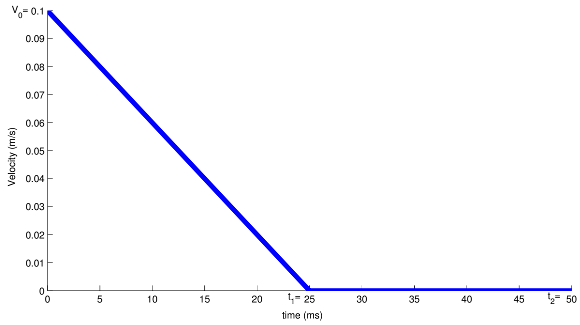

Fig. 1. Time evolution of the skull velocity

The model will use three-dimension linear wedge elements (C3D6) and a prony series particles both included in the library of the commercial software.

1.4 Our Approximation

The approximation that have been taken into account in these study is only taking into account the brain and the CSF as different parts, also using an Ogden and Monney-Rivlin hyperelastic formulations, in order to validate the use of the 3D thin slices using all the specifications previously mentioned in these section, the validation will be made using the whole model of the rat brain computed by F. Casadei et al. [13,14,15] using the EUROPLEXUS software.

The brain matter is considered as an isotropic viscoelastic material modeled with a prony series approximation for the time-dependent behaviour, while the CSF is taken as a fluid-like material without viscosity and modeled with finite elements (figure 2).

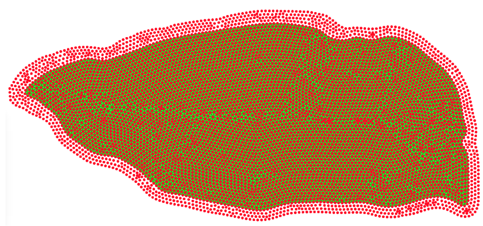

Fig. 2. Geometry with the differentiation of the brain matter (inner part), and the CSF (outer part)

2. THE MODEL

For the discretization of the material an hyperelastic material is defined, non-linear and isotropic due to that in Abaqus all hyperelastic models are based on the assumptions of isotropic behavior throughout the deformation history.

2.1 Hyper-elasticity

Hyperelastic materials are described in terms of a strain energy potential, $U(\varepsilon)$, which defines the strain energy stored in the material per unit of reference volume (volume in the initial configuration) as a function of the strain at that point in the material. There are several forms of strain energy potentials available in Abaqus to model approximately incompressible isotropic elastomers.

Two hyperelastic materials are used in the simulations, the Mooney-Rivlin and the Ogden forms, because even if are usually used on the cases of rubber-like materials nowadays are widely used in biological tissue-like materials.

The Ogden strain energy potential form is:

$$U = \sum_{i=1}^{N} \frac{2\mu_i}{\alpha_i^2}(\bar{\lambda}_1^{\alpha_i} + \bar{\lambda}_2^{\alpha_i} + \bar{\lambda}_3^{\alpha_i} - 3) + \sum_{i=1}^{N} \frac{1}{D_i}(J^{el} - 1)^2 \quad (1)$$

where U is the strain energy per unit of reference volume; $\bar{\lambda}_i$ are the deviatoric principal stretches; λ_i are the principal stretches; μ_i, α_i, and $D_i$are temperature-dependent material parameters; J^{el} is the elastic volume ratio; μ_0 the initial shear modulus and K_0 the initial bulk modulus .

$$\bar{\lambda}_i = J^{-1/3}\lambda_i \quad (2)$$

$$\mu_0 = \sum_{i=1}^{N} \mu_i \quad and \quad K_0 = 2/D_1 \quad (3)$$

The Mooney-Rivlin strain energy potential form is:

$$U = C_{10}(\mathbf{I}_1 - 3) + C_{01}(\mathbf{I}_2 - 3) + \frac{1}{D_1}(J^{el} - 1)^2 \quad (4)$$

Where C_{10}, C_{01} and D_1 are temperature-dependent material parameters; $\bar{I}_1$ and $\bar{I}_2$ are the first and second deviatoric strain invariants.

$$\bar{I}_1 = \bar{\lambda}_1^2 + \bar{\lambda}_2^2 + \bar{\lambda}_3^2 \quad and \quad \bar{I}_2 = \bar{\lambda}_1^{-2} + \bar{\lambda}_2^{-2} + \bar{\lambda}_3^{-2} \quad (5)$$

$$\mu_0 = 2(C_{10} + C_{01}) \quad and \quad K_0 = 2/D_1 \quad (6)$$

2.2 Prony series

For the numerical implementation of the fluid like material CSF (white matter) a Prony series has been used. The continuum particle elements (PC3D) are useful for simulations involving material that undergoes extreme deformation and are defined using only one node; however, the element centered at a given node (particle) receives contributions from all particles within a sphere of influence whose radius is commonly referred to as the smoothing length. The smoothed particle hydrodynamic (SPH) formulation determines at every increment of the analysis the connectivity associated with a given particle. Since nodal connectivity is not fixed, severe element distortion is avoided and, hence, the formulation allows for very high strain gradients.

2.3 Viscoelasticity

After a preliminary study to calibrate the temperature-dependent parameters by the hyperelastic analysis the time domain Viscoelasticity is implemented. The model describes an isotropic rate-dependent material behavior for materials in which dissipative losses primarily caused by viscous (internal damping) effects must be modeled in the time domain and assumes that the shear (deviatoric) and volumetric behaviors are independent in multiaxial stress states.

3. RESULTS

A series of numerical simulations is performed by using the head slices described in the previous section. Some similar calculations had already been performed in references[13,14,15]. The difference is that the simulations of that references are computed with the software EUROPLEXUS[4] with a full brain model and without considering the prony series, and also it gives rise to the idea of implement the use of the slice meshes. Also these papers will be used to verify our model by using the same values of the material and comparing the numerical results.

[4]Computer code jointly developed by the French Commissariat à l'Energie Atomique (CEA DMT Saclay) and by EC-JRC.

Table I . Experimental values used for the validation

		μ_1	α_1	μ_2	α_2	D
Ogden *N=2*						
	Brain	-0.29	-10.8	9.6E-3	19.7	2E-4
	CSF	-0.0029	-10.8	9.6E-5	19.7	2E-6
Mooney-Rivlin		C_{10}		C_{01}		D_1
	Brain	185		46.3		2E+4
	CSF	185E-2		46.3E-2		2E+6

We start by performing calculations of the rat head slices with both methods using the data parameters defined in the Table I .

Once the *Ogden* hyperelastic case is computed, it gives results while displaying the warning that the hyperelastic material is unstable, with:

- Uniaxial tension: unstable for all strains
- Uniaxial compression: unstable for all strains
- Biaxial tension: unstable for all strains
- Biaxial compression: unstable for all strains
- Planar tension: unstable for all strains
- Planar compression: unstable for all strains
- Volumetric tension: stable for all volume ratios
- Volumetric compression: stable for all volume ratios

On the other hand, when the $Mooney - Rivlin$ case is computed arriving at the chosen final time of 50 ms in 5001 Increments.

The next Figures depicts the longitudinal stress (σ_{yy}) distributions at different time steps, and from those two distinct phases can be identified. The first phase until the end of the deceleration $t = 25md$ in which the brain matter is compressed in the dorso and having the frontal part under traction while the central part is relatively stress-free.

The second phase is the one for $t > 25ms$ where the skull is held fixed. During these phase the previous oscillatory pattern is broken appearing cycles of traction and compression.

Those Figures where used to make a comparison with the ones of the full 3D model[14,15]. The good agreement between the slices and the full 3D model, at least until the end of the deceleration phase, is very promising in the way of using the slices as a preliminary cheap simulations.

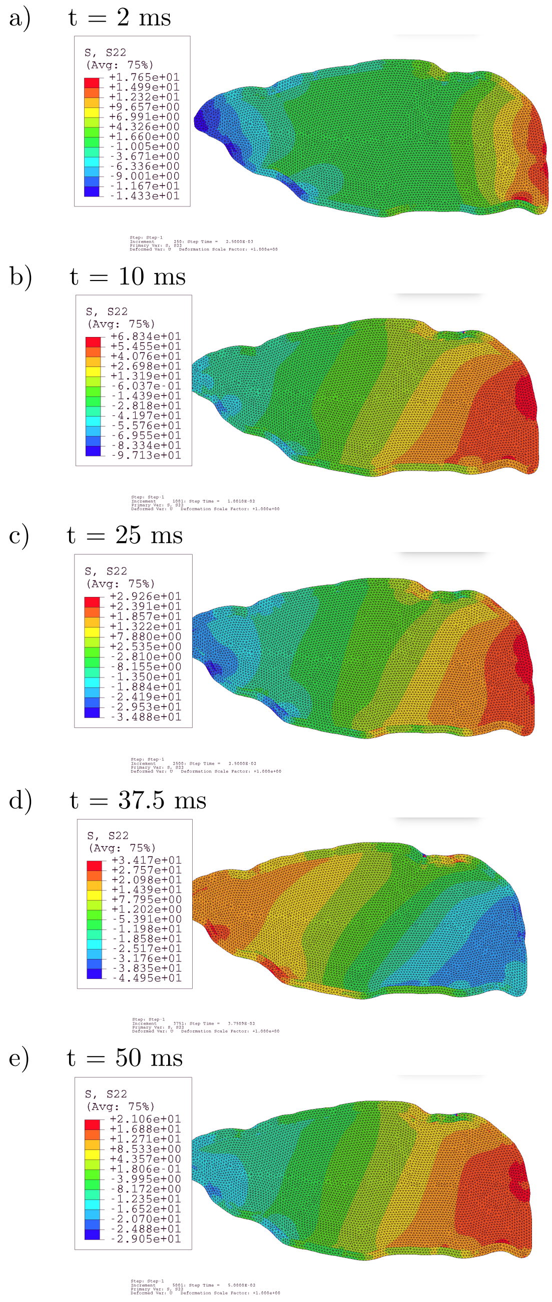

Fig. 3. Longitudinal stress in rat head slices in the Mooney-Rivlin case.

4. CONCLUSIONS

As a concluding remark it has to be said that the validation of the Mooney-Rivlin model has been done. Regarding for the Ogden hyperelastic model, which is unstable under that material data with Abaqus 6.14 is left as a future work the validation of that model.

ACKNOWLEDGMENTS

This research is supported by the European Joint Research Center in Ispra (Itally). We thank one of the reviewers for many helpful comments.

Referencias

1. Rika M. Wright, K. T. Ramesh. An axonal strain injury criterion for traumatic brain injury. Biomech Model Mechanobiol, 2012; 11:245-260.
2. Rika M. Wright, Andrew Post, Blaine Hoshizaki, Kaliat T. Ramesh. A Multiscale Computational Approach to Estimating Axonal Damage under Inertial Loading of the Head. Journal of neurotrauma, 2013; 30:102-118.
3. Yuan Feng, Ruth J.Okamoto, Ravi Namani, Guy M. Genin, Philip V. Bayly. Measurements of mechanical anisotropy in brain tissue and implications for transversely isotropic material models of white matter. Journal of the mechanical behavior of biomedical materials, 2013, 117-132
4. T. Kaster, I. Sack, A. Samani. Measurement of the hyperelastic properties of ex vivo brain tissue slices. Journal of Biomechanics 44, 2011, 1158-1163
5. Thibault P. Prevost, Guang Jin, Marc A. de Moya, Hasan B. Alam, Subra Suresh, Simona Socrate. Dynamic mechanical response of brain tissue in indentation in vivo, in situ and in vitro. Acta Biomaterialista 7, 2011, 4090-4101
6. Y. Feng, T. M. Abney, R. J. Okamoto, R. B. Pless, G. M. Genin, P. V. Bayly. Relative brain displacement and deformation during constrained mild frontal head impact. Journal of the royal society interface 7, 2010, 1677-1688
7. J.A.W. van Dommelen, T.P.J. van der Sande, M. Hrapko, G.W.M. Peters. Mechanical properties of brain tissue by indentation: Interregional variation. Journal of the mechanical behavior of biomedical materials 3, 2010, 158-166.
8. Rijk de Rooij, Ellen Kuhl. Constitutive Modelling of Brain Tissue: Current Perspectives. Applied Mechanics Reviews, 2016, 010801-1
9. Linxia Gu, Mehdi S. Chafi, Shailesh Ganpule, Namas Chandra. The influence of Heterogeneous Menings on the Brain mechanics under Primary Blast Loading. Mechanical materials Engineering Faculty Publications. Paper 83 (2012)
10. Silvia Budday, Richard Nay, Rijk de Rooij, Paul Steinmann, Thomas Wyrobek, Timothy C. Ovaert, Ellen Kuhl. Mechanical properties of gray and white matter brain tissue by indentation. journal of the mechanical behavior of biomedical materials 46 (2015) 318 330
11. Badar Rashid, Michael Destrade, Michael Gilchrist. Mechanical Characterisation of Brain Tissue in comparison at Dynamic Strain Rates.
12. Prange MT, Margulies SS. Regional, directional and age-dependentproperties of the brain undergoing large deformation. J. Biomech Eng Trans Asme,2002) 124(2):244-252. doi:10.1115/1. 1449907
13. F. Casadei, P. Saez, P. Díez, M. Larcher, G. Valsamos. Scoping calculations for simulation of human head impact with EUROPLEXUS. JRC Technical Report, in publication.
14. F. Casadei, P. Saez, P. Díez, M. Larcher, G. Valsamos. Simulation of rat head deceleration with EUROPLEXUS. JRC Technical Report, in publication.
15. F. Casadei, P. Saez, P. Díez, M. Larcher, G. Valsamos. Simulation of rat and monkey head slice deceleration with EUROPLEXUS. JRC Technical Report, in publication.
16. Holzapfel G.A.-Nonlinear Solid Mechanics$_A Continuum approach for engineering$(2000)
17. Abaqus User's Manual, on-line version: http://bobcat.nus.edu.sg:2080/v6.14/index.html